Pure & Appl. Chem., Vol. 67, No. 2, pp. 323–330, 1995.
Printed in Great Britain.

Structural aspects of the redox flexibility of group VIII metal complexes with tripodal polyphosphine ligands

Piero Zanello
University of Siena, Department of Chemistry, Piano dei Mantellini 44, 53100 Siena, Italy

Abstract: Complexes of transition metal fragments with tripodal polyphosphine ligands (*NP_3*, *PP_3*, *triphos*) usually display reversible electron-transfer processes. Sometimes, such derivatives undergo electron addition/removal steps which cause more or less complicated molecular reorganizations. A few examples of these redox-induced rearrangements are here illustrated.

In recent years we have widely documented the remarkable aptitude of tripodal polyphosphines, either in the tetradentate *NP_3* and *PP_3* form or in the tridentate *triphos* assembly (Scheme 1), to stabilize mono- and (homo-/hetero-)bi-nuclear metal complexes capable of undergoing multiple and reversible electron-transfer processes. As a result, the central metal ion [iron (1,2), cobalt (1,3-8), rhodium (1,4,9-21), iridium (4,8), nickel (4,22,23)] often accedes to unusual oxidation states.

SCHEME 1

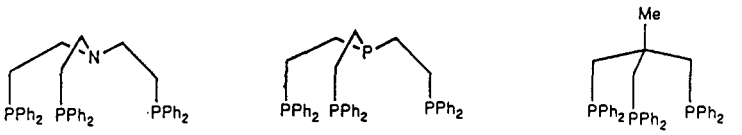

NP_3 PP_3 triphos

Nevertheless, in some cases, these complexes display electron addition/removal processes able to trigger significant molecular rearrangements of the original framework. We wish here to give prominence just to this redox-induced reorganizational aspect, not only to complete the picture of the redox flexibility of this class of polyphosphine-metal complexes, but also in the hope of showing how electrochemistry can offer an easy way to detect more or less complicated chemical pathways.

All the potential values here cited are referred to the Saturated Calomel Electrode (S.C.E.).

Oxidatively-induced conversion of [(PP$_3$)M(H)Cl] into [(PP$_3$)MCl]$^+$ (M=Fe,Ru,Os)

The conversion of [(PP$_3$)M(H)Cl] into [(PP$_3$)MCl]$^+$ (M=Fe,Ru,Os), which is outlined in Scheme 2, follows different electrode pathways depending upon the central metal atom (24).

SCHEME 2

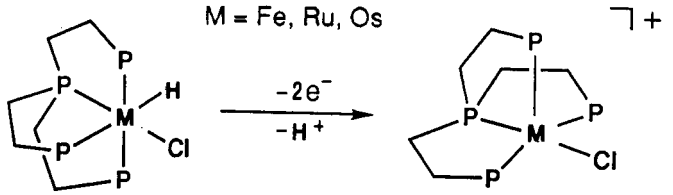

As a representative example, we report here the conversion process of a ruthenium(II) complex. Figure 1 shows that the chloride-hydride Ru(II) complex undergoes an irreversible (two-electron) oxidation, which generates in the reverse scan a voltammetric profile quite coincident with that of the chloride Ru(II) monocation. The electrochemical results testify the following electrode path:

$$(PP_3)Ru(H)Cl \xrightarrow{-2e} [(PP_3)Ru(H)Cl]^{2+} \xrightarrow[-H^+]{t_{1/2} \approx 0.5\ sec} [(PP_3)RuCl]^+$$

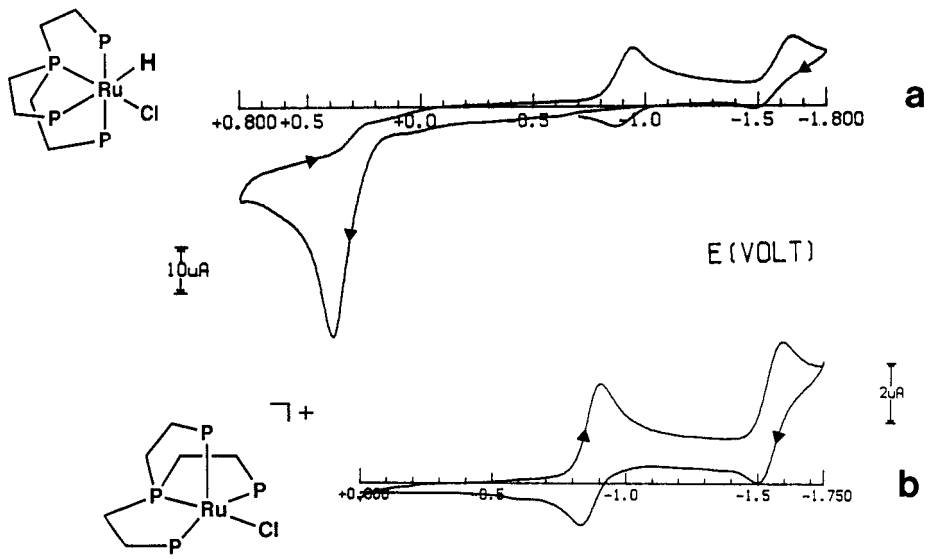

Fig.1 *Cyclic voltammograms recorded at a platinum electrode on deaerated THF solutions containing [NBu$_4$](ClO$_4$) (0.2 mol dm^{-3}) and: (a) [(PP$_3$)Ru(H)Cl]; scan rate 0.5 Vs^{-1}; (b) [(PP$_3$)RuCl](BPh$_4$); scan rate 0.02 Vs^{-1}.*

As a consequence of the octahedral-to-square pyramidal reorganization following the deprotonation process, the Ru-Cl bond shortens by about 0.1 Å (from 2.52 Å to 2.43 Å), whereas the *trans* Ru-P bond elongates by 0.05 Å (from 2.19 Å to 2.24 Å).

Oxidatively-induced conversion of $[(PP_3)Co(H_2)]^+$ into $[(PP_3)CoH]^+$

As illustrated in Scheme 3, the anodically promoted conversion of the "nonclassical" dihydrogen Co(I) cation $[(PP_3)Co(H_2)]^+$ to the corresponding Co(II) monohydride cation $[(PP_3)CoH]^+$ also involves a deprotonation step (5).

SCHEME 3

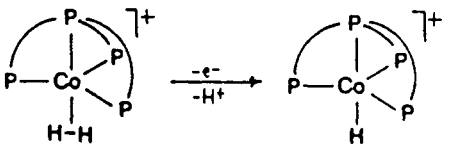

As a matter of fact, Figure 2 proves that the irreversible (one-electron) oxidation of $[(PP_3)Co(H_2)]^+$ produces $[(PP_3)CoH]^+$, in that the backresponse originated from this anodic process is quite complementary to the one-electron oxidation profile exhibited by the Co(I) complex $[(PP_3)CoH]$.

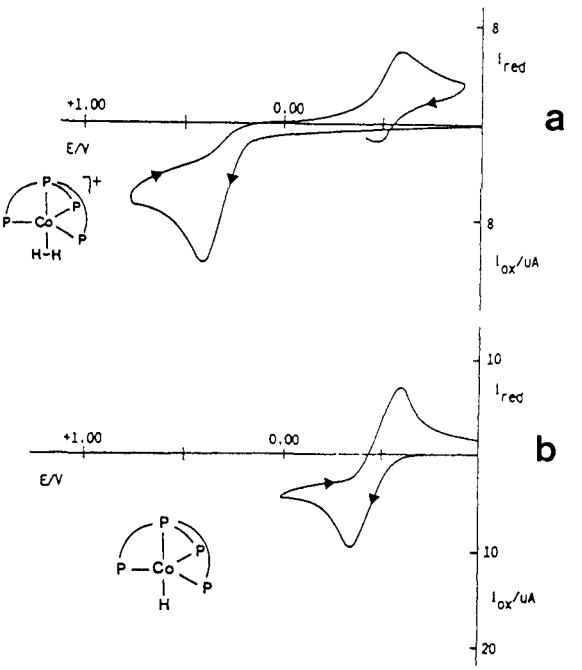

Fig.2

Cyclic voltammetric responses recorded on deaerated THF solutions containing $[NBu_4][ClO_4]$ (0.2 mol dm^{-3}) and: (a) $[(PP_3)Co(H_2)]^+$; (b) $[(PP_3)CoH]$. Scan rate 0.2 Vs^{-1}. Platinum working electrode.

In the solid state, the averaged equatorial Co-P distance, which is 2.20 Å in the dihydrogen cation, shortens by about 0.02 Å in the monohydride cation; correspondingly, the apical Co-P distance

elongates by 0.04 Å (from 2.12 Å to 2.16 Å).

Indeed, from the stereochemical viepoint this conversion is somewhat less simple than is expected, in that spectroscopic evidence proves it to involve the trigonal bipyramidal -to-square pyramidal geometrical change depicted in Scheme 4.

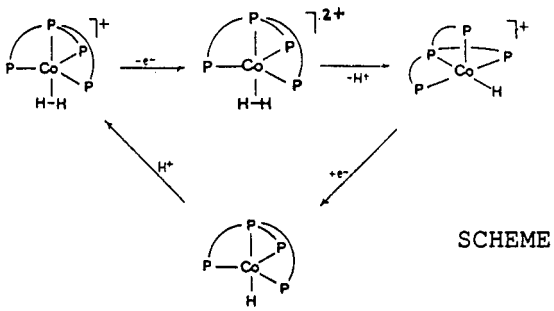

SCHEME 4

Redox-induced conversion of $[(XP_3)M\{C{=}CH(Ph)\}]^+$ into $[(XP_3)M(C{\equiv}CPh)]^{n+}$ (X=N,P; M=Co,Rh; n=0,2)

We have shown that the M(I)-vinylidene complexes $[(XP_3)M\{C{=}CH(R)\}]^+$ (X=N,P; M=Co,Rh; R=Ph,COOEt) convert to the related σ-alkynyl complexes $[(XP_3)M(C{\equiv}CR)]^{n+}$ [n=0, M(I); n=2, M(III)] through simple electron-transfer processes (6,17). A clear picture of such reorganization is illustrated in Figure 3, which refers to the $[(NP_3)Rh\{C{=}CH(Ph)\}]^+/[(NP_3)Rh(C{\equiv}CPh)]^{n+}$ (n=0,2) systems.

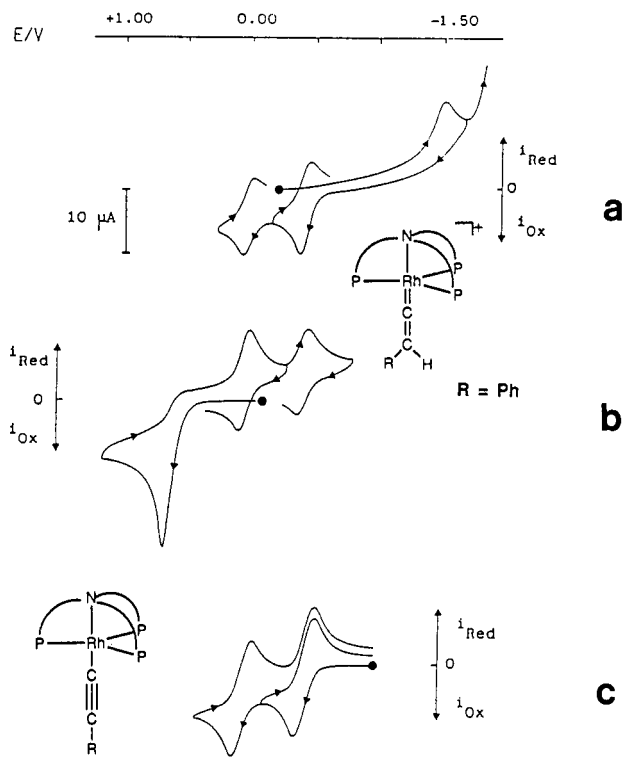

Fig.3
Cyclic voltammetric responses recorded on deaerated CH_2Cl_2 solutions containing $[NBu_4](ClO_4)$ (0.2 mol dm^{-3}) and: (a,b) $[(NP_3)Rh\{C{=}CH(Ph)\}]^+$; (c) $[(NP_3)Rh(C{\equiv}CPh)]$. Scan rate 0.2 Vs^{-1}. Platinum working electrode.

It is well evident that either a two-electron oxidation (Figure 3b) or a one-electron reduction (Figure 3a) of the vinylidene monocation $[(NP_3)Rh\{C{=}CH(Ph)\}]^+$ afford the σ-alkynyl congeners $[(NP_3)Rh(C{\equiv}CPh)]^{n+}$ (n = 2, 0, respectively), according to the pathway shown in Scheme 5.

SCHEME 5

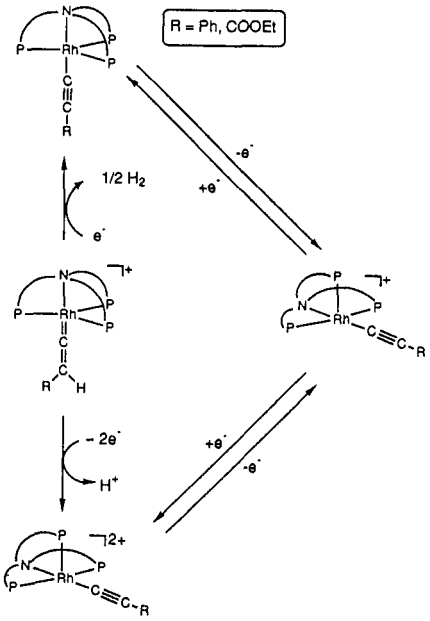

Redox-induced reversible migration of hydrogen from a metal centre to a peripheral alkene ligand

A path more intriguing than the previously discussed removals of hydrogen atoms is involved in the redox-induced reversible transformation of the octahedral Rh(I) hydride-dimethyl fumarate $(triphos)RhH(MeO_2CCH{=}CHCO_2Me)$ into the related Rh(III) succinyl dication $[(triphos)Rh\{CH(CO_2Me)CH_2(CO_2Me)\}]^{2+}$ (13), Scheme 6.

SCHEME 6

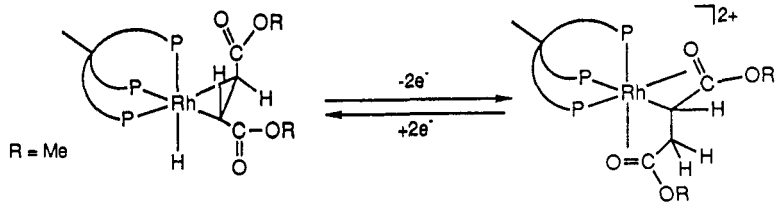

As illustrated in Figure 4, the hydride-dimethyl fumarate complex undergoes an irreversible (two-electron) oxidation which generates in the reverse scan a reduction profile quite coincident with that of the succinyl dication. As a matter of fact, the latter species undergoes a first reversible one-electron reduction, followed by a second irreversible step, which in turn exhibits in the reverse scan the oxidation peak of the original dimethyl-fumarate complex. The overall interconversion path is depicted in Scheme 7.

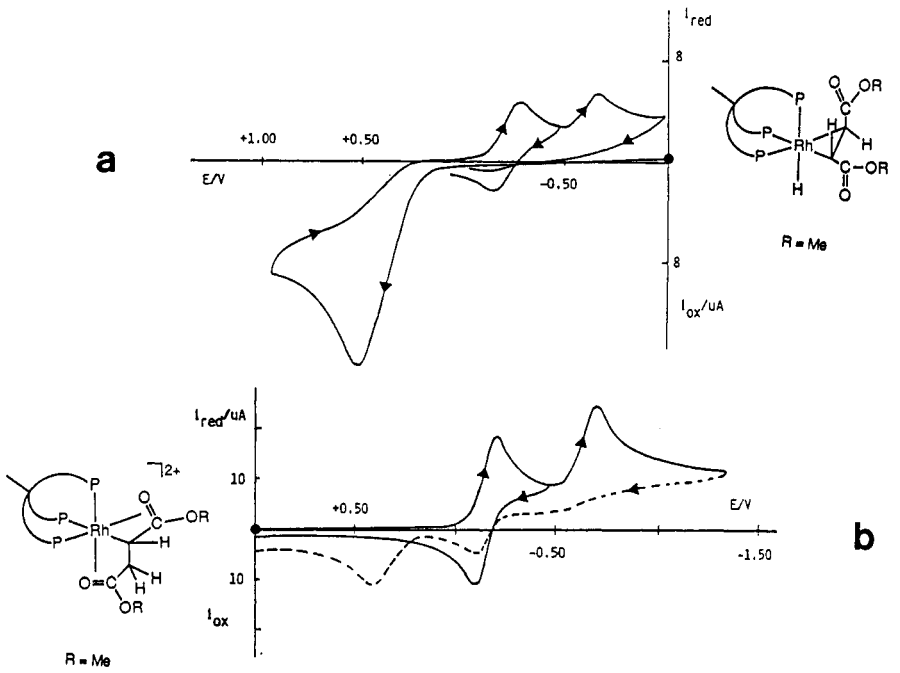

Fig.4 *Cyclic voltammograms recorded at a platinum electrode on: (a) THF solution of [(triphos)RhH(MeO$_2$CCH=CHCO$_2$Me)]; (b) CH$_2$Cl$_2$ solution of [(triphos)Rh{CH(CO$_2$Me)CH$_2$(CO$_2$Me)}]$^{2+}$. [NBu$_4$][ClO$_4$] (0.2 mol dm^{-3}) supporting electrolyte. Scan rate 0.2 Vs^{-1}.*

SCHEME 7

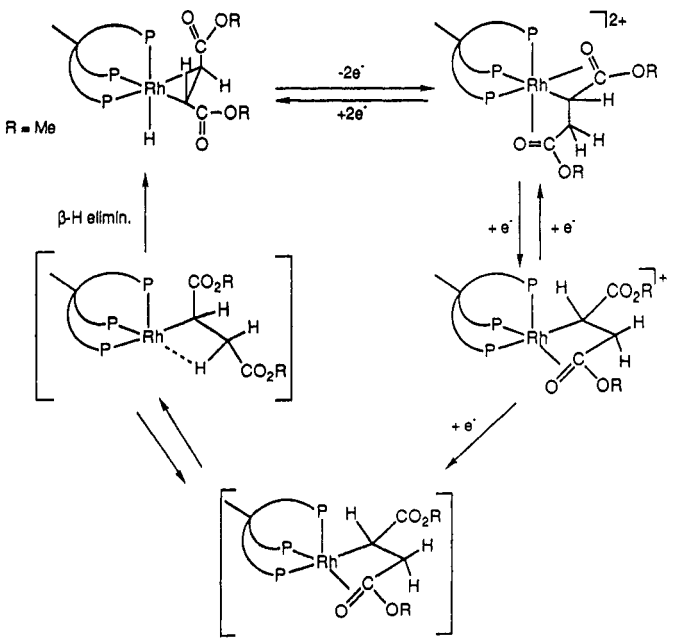

Redox induced interconversion of $\mu(\eta^2,\eta^2)$-ethynyldirhodium(III) into $\mu(\eta^1,\eta^1)$-ethynyldirhodium(III) complex

As a last example of redox-induced reorganizational process, we report the reversible orientation of an acetylene group bridging two Rh(III) fragments from *perpendicular* to *parallel* disposition which occurs in the anodic oxidation of [(triphos)Rh(μ-Cl)(μ-η^2,η^2-C_2H_2)Rh(triphos)]Cl to [(triphos)Rh(μ-Cl)$_2$(μ-η^1,η^1-C_2H_2)Rh(triphos)]$^{2+}$ (20), Scheme 8.

SCHEME 8

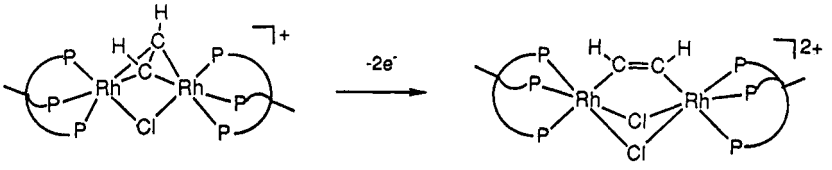

As shown in Figure 5, the *perpendicular* monocationic complex undergoes an irreversible (two-electron) oxidation which generates in the reverse scan a voltammetric profile quite coincident with that of the *parallel* dication.

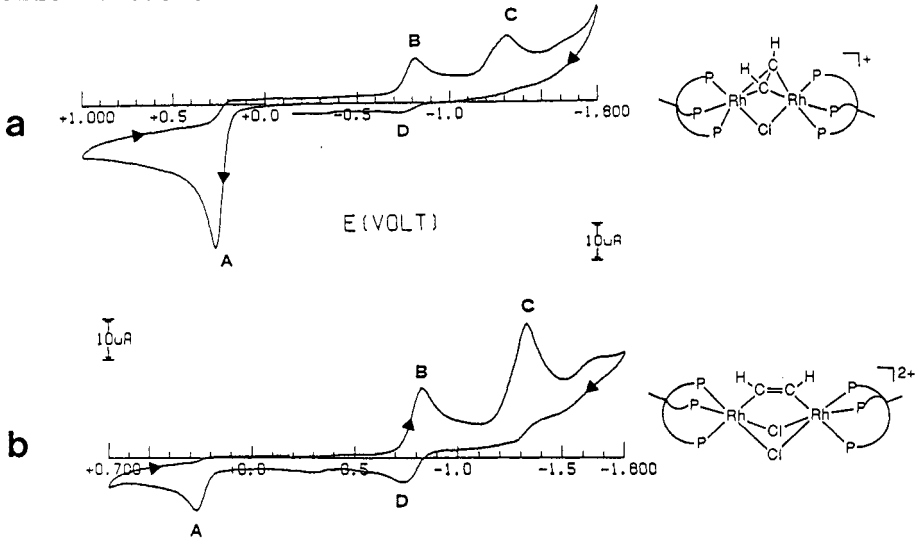

Fig.5 *Cyclic voltammograms recorded at a platinum electrode on CH_2Cl_2 solutions of: (a) [(triphos)Rh(Cl)(C_2H_2)Rh(triphos)]Cl; (b) [(triphos)Rh(Cl)$_2$(C_2H_2)Rh(triphos)](ClO_4)$_2$. [NBu_4][ClO_4] (0.2 mol dm^{-3}) supporting electrolyte. Scan rate 0.2 Vs^{-1}.*

An accurate examination of the electrochemical data allowed us to shed light on the intimate mechanism of the overall process, which can be depicted according to the EC_aC_rE mechanism illustrated in Scheme 9 (C_a = chloride association; C_r = geometrical reorganization).

SCHEME 9

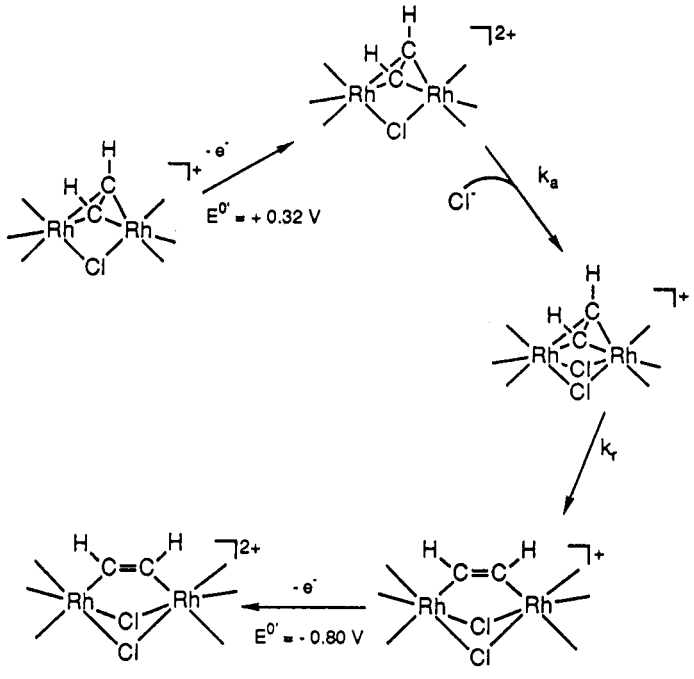

References

1. C.Bianchini *et al. J.Am.Chem.Soc.* **110**, 3913 (1988).
2. C.Bianchini *et al. J.Am.Chem.Soc.* **115**, 2723 (1993).
3. C.Bianchini *et al. Inorg.Chem.* **26**, 3683 (1987).
4. C.Bianchini *et al. Inorg.Chem.* **28**, 2552 (1989).
5. C.Bianchini *et al. Inorg.Chem.* **29**, 3394 (1990).
6. C.Bianchini *et al. Organometallics* **9**, 2514 (1990).
7. M.Di Vaira *et al. Polyhedron* **10**, 2123 (1991).
8. P.Barbaro *et al. Inorg.Chim.Acta* **198-200**, 31 (1992).
9. C.Bianchini *et al. J.Am.Chem.Soc.* **109**, 185 (1987).
10. C.Bianchini *et al. Inorg.Chem.* **26**, 3677 (1987).
11. C.Bianchini *et al. Organometallics* **7**, 1660 (1988).
12. F.Cecconi *et al. J.Organomet.Chem.* **353**, C5 (1988).
13. S.Bianchini *et al. Organometallics* **7**, 2575 (1988).
14. C.Bianchini *et al. Inorg.Chem.* **27**, 4429 (1988).
15. C.Bianchini *et al. Inorg.Chem.* **28**, 227 (1989).
16. C.Bianchini *et al. Organometallics* **8**, 893 (1989).
17. C.Bianchini *et al. Organometallics* **9**, 241 (1990).
18. C.Bianchini *et al. Organometallics* **9**, 360 (1990).
19. C.Bianchini *et al. Inorg.Chem.* **29**, 3402 (1990).
20. C.Bianchini *et al. Organometallics* **10**, 636 (1991).
21. C.Bianchini *et al. Topics in Physical Organometallic Chemistry*, Vol.4, p.139, Freund Publishing House, London (1992).
22. C.A.Ghilardi *et al. Struct.Chem.* **1**, 441 (1990).
23. P.Zanello *et al. J.Chem.Soc., Dalton Trans.* 3761 (1990).
24. C.Bianchini *et al.* manuscript in preparation.